Exact exchange potential for slabs: Asymptotic behavior of the Krieger-Li-Iafrate approximation

Eberhard Engel

Center for Scientific Computing, J. W. Goethe-Universität Frankfurt, Max-von-Laue-Strasse 1, D-60438 Frankfurt am Main, Germany

(Received 13 December 2017; published 1 February 2018)

The Krieger-Li-Iafrate (KLI) approximation for the exact exchange (EXX) potential of density functional theory is investigated far outside the surface of slabs. For large z the Slater component of the EXX/KLI potential falls off as $-1/z$, where z is the distance to the surface of a slab parallel to the xy plane. The Slater potential thus reproduces the behavior of the exact EXX potential. Here it is demonstrated that the second component of the EXX/KLI potential, often called the orbital-shift term, is also proportional to $1/z$ for large z, at least in general. This result is obtained by an analytical evaluation of the Brillouin zone integrals involved, relying on the exponential decay of the states into the vacuum. Several situations need to be distinguished in the Brillouin zone integration, depending on the band structure of the slab. In all standard situations, including such prominent cases as graphene and Si(111) slabs, however, a $1/z$ dependence of the orbital-shift potential is obtained to leading order. The complete EXX/KLI potential therefore does not reproduce the asymptotic behavior of the exact EXX potential.

DOI: 10.1103/PhysRevB.97.075102

I. INTRODUCTION

Density functional approaches utilizing the exact exchange (EXX) often yield clear improvements over conventional density functionals, such as the local-density approximation (LDA) or the generalized gradient approximation (GGA), and are therefore more and more routinely used in electronic structure calculations [1–24] (for an overview of the EXX approach see Refs. [25,26]). The self-consistent application of the EXX suffers from the high computational cost involved in determining the corresponding EXX potential v_x by the optimized (effective) potential method (OPM) [27]. For this reason, often, the Krieger-Li-Iafrate (KLI) approximation [28] for v_x is employed, which allows us to perform self-consistent EXX calculations much more efficiently. The KLI approximation has been found to be quite accurate in a variety of situations, including not only electronic structure calculations for atoms [29,30], molecules [31–34], and solids [22,23,35] but also time-dependent problems [36] (however, also some failures have been reported [9,37–39]). Recently, the KLI approximation was also applied in EXX calculations for slabs [40,41]. Both in the case of a quasi-two-dimensional electron gas [41] and for graphene [40] the KLI potential v_x^{KLI} turned out to be quite close to the exact EXX potential obtained by the OPM.

The success of the KLI approximation partially stems from the fact that v_x^{KLI} reproduces the behavior of the exact v_x in the asymptotic region of atoms and other finite systems. For a large distance r from the nucleus the atomic EXX potential [27] falls off as $v_x \sim -1/r$, which reflects the self-interaction correction provided by the EXX functional. Simultaneously, the corresponding EXX energy density e_x is asymptotically proportional to $-n/(2r)$, where n is the electron density. As a result, the Slater potential $v_{\mathrm{Slater}} = 2e_x/n$, the first component of v_x^{KLI},

$$v_x^{\mathrm{KLI}} = v_{\mathrm{Slater}} + v_{\mathrm{shift}},$$

behaves exactly as the exact v_x. At the same time, the second component of v_x^{KLI}, the orbital-shift potential v_{shift}, often even decays exponentially for large r (in particular for closed-subshell atoms). Analogous relations for the exact v_x and e_x have also been derived for slabs, both on the basis of the jellium model [42–46] and for nonjellium slabs [40,47]. At a large distance z from the surface of the slab (assumed to be parallel to the xy plane) the exact v_x falls off as $-1/z$, while $e_x \sim -n/(2z)$. Again, the Slater potential reproduces the asymptotic behavior of v_x, $v_{\mathrm{Slater}} \sim -1/z$.

In the present contribution the behavior of v_{shift} far outside the surface of a slab is analyzed on the basis of an analytical evaluation of the Brillouin zone (BZ) integrals involved. This analysis reveals that v_{shift} does not decay rapidly into the vacuum, even though $v_{\mathrm{shift}}(z \to \infty) = 0$ is ensured by suitable normalization (use of the analytical form of the Bloch states in the vacuum allows an extrapolation of the potential to $z = \infty$). Rather, one finds a $1/z$ behavior of v_{shift} for large z, at least in general.

The analytical BZ integration utilizes the asymptotic form of the Bloch states. The exponential decay of these states is controlled by their band energies. In the BZ integration one therefore has to distinguish several situations, depending on the properties of the band structure. For most types of band structures the BZ integrations can be performed with a technique inspired by the saddle-point approximation. While the asymptotic behavior of the individual components of v_{shift} depends on the particular band structure, a $1/z$ dependence is found for the asymptotic v_{shift} in most situations. As a consequence, the total v_x^{KLI} does not decay as $-1/z$ in the asymptotic region.

This paper is organized as follows: In Sec. II the KLI approximation for an arbitrary slab is specified in detail, addressing in particular the behavior of the KLI exchange potential for large z. The analytical BZ integration over the asymptotic states of the slab is discussed in Sec. III. The

integration is performed for a generic expression of the type relevant for $v_{\rm shift}$, so that the results can also be useful in other contexts. Section IV then applies the results of Sec. III to $v_{\rm shift}$. A brief discussion of the range of z for which the present results can be expected to be valid concludes the paper (Sec. V). Atomic units are used throughout this work.

II. KLI APPROXIMATION TO THE EXACT EXCHANGE POTENTIAL OF SLABS

A slab is characterized by a total KS potential $v_{\rm s}$ which is periodic in the xy directions but confines the electrons to the finite range $-L < z < L$ in the z direction,

$$v_{\rm s}(\boldsymbol{r}) = \sum_{\boldsymbol{G}} e^{i\boldsymbol{G}\cdot\boldsymbol{r}_\parallel} v(\boldsymbol{G},z). \tag{1}$$

Here $\boldsymbol{r}_\parallel = (x,y)$, and $\boldsymbol{G}$ is a vector of the two-dimensional (2D) reciprocal lattice in the xy directions. The corresponding KS states have the form

$$\phi_{\boldsymbol{k}\alpha}(\boldsymbol{r}) = \frac{e^{i\boldsymbol{k}\cdot\boldsymbol{r}_\parallel}}{\sqrt{A}} \sum_{\boldsymbol{G}} e^{i\boldsymbol{G}\cdot\boldsymbol{r}_\parallel} c_{\boldsymbol{k}\alpha}(\boldsymbol{G},z), \tag{2}$$

where $\boldsymbol{k}$ is the 2D crystal momentum and A is the area of the 2D unit cell. Assuming the slab is spin saturated, the electron density of the slab is given by

$$n(\boldsymbol{r}) = 2A \int_{\rm 1BZ} \frac{d^2k}{(2\pi)^2} \sum_\alpha \Theta_{\boldsymbol{k}\alpha} |\phi_{\boldsymbol{k}\alpha}(\boldsymbol{r})|^2, \tag{3}$$

with $\Theta_{\boldsymbol{k}\alpha}$ denoting the occupation of the state $\boldsymbol{k}\alpha$. The $\boldsymbol{k}$ integration extends over the first BZ.

The KLI approximation [28] for the exact exchange potential consists of two contributions, the Slater term and the orbital-shift term,

$$v_{\rm x}^{\rm KLI}(\boldsymbol{r}) = v_{\rm Slater}(\boldsymbol{r}) + v_{\rm shift}(\boldsymbol{r}). \tag{4}$$

The Slater potential is determined by the EXX energy density $e_{\rm x}(\boldsymbol{r})$,

$$v_{\rm Slater}(\boldsymbol{r}) = 2\,\frac{e_{\rm x}(\boldsymbol{r})}{n(\boldsymbol{r})}. \tag{5}$$

In the case of spin-saturated slabs the EXX energy density can be expressed as

$$e_{\rm x}(\boldsymbol{r}) = A \int_{\rm 1BZ} \frac{d^2k}{(2\pi)^2} \sum_\alpha \Theta_{\boldsymbol{k}\alpha}\, e_{{\rm x},\boldsymbol{k}\alpha}(\boldsymbol{r}), \tag{6}$$

$$e_{{\rm x},\boldsymbol{k}\alpha}(\boldsymbol{r}) = -A \int_{\rm 1BZ} \frac{d^2k'}{(2\pi)^2} \sum_{\alpha'} \Theta_{\boldsymbol{k}'\alpha'} \int d^3r' \times \frac{\phi^*_{\boldsymbol{k}\alpha}(\boldsymbol{r})\phi_{\boldsymbol{k}'\alpha'}(\boldsymbol{r})\phi^*_{\boldsymbol{k}'\alpha'}(\boldsymbol{r}')\phi_{\boldsymbol{k}\alpha}(\boldsymbol{r}')}{|\boldsymbol{r}-\boldsymbol{r}'|}. \tag{7}$$

The orbital-shift potential for slabs has the form

$$v_{\rm shift}(\boldsymbol{r}) = \frac{2\,A}{n(\boldsymbol{r})} \int_{\rm 1BZ} \frac{d^2k}{(2\pi)^2} \sum_\alpha \Theta_{\boldsymbol{k}\alpha} \Delta_{\boldsymbol{k}\alpha} |\phi_{\boldsymbol{k}\alpha}(\boldsymbol{r})|^2, \tag{8}$$

with

$$\Delta_{\boldsymbol{k}\alpha} = \int_A d^2r_\parallel \int_{-\infty}^{\infty} dz \left[|\phi_{\boldsymbol{k}\alpha}(\boldsymbol{r})|^2 v_{\rm x}^{\rm KLI}(\boldsymbol{r}) - e_{{\rm x},\boldsymbol{k}\alpha}(\boldsymbol{r})\right]. \tag{9}$$

If the normalization of $v_{\rm s}$ is chosen accordingly, the total KS potential far outside the surface of the slab behaves as

$$v_{\rm s}(\boldsymbol{r}) \xrightarrow{z\gg L} -\frac{u}{z}. \tag{10}$$

Depending on the choice for the exchange-correlation functional, u may vanish (LDA/GGA), $u = 1$ (if the exact $v_{\rm x}$ is combined with a short-range correlation potential), or u assumes some value between 0 and 1. An analysis of the KS equations with the potential (10) shows that, to leading order, the Fourier coefficients of the states (2) asymptotically decay as [47]

$$c_{\boldsymbol{k}\alpha}(\boldsymbol{G},z) \xrightarrow{z\gg L} f_{\boldsymbol{k}\alpha}(\boldsymbol{G})\, z^{u/\gamma_{\boldsymbol{k}\alpha}(\boldsymbol{G})}\, e^{-\gamma_{\boldsymbol{k}\alpha}(\boldsymbol{G})z}, \tag{11}$$

with

$$\gamma_{\boldsymbol{k}\alpha}(\boldsymbol{G}) = [(\boldsymbol{G}+\boldsymbol{k})^2 - 2\epsilon_{\boldsymbol{k}\alpha}]^{1/2}. \tag{12}$$

Here $\epsilon_{\boldsymbol{k}\alpha}$ is the KS eigenenergy of the state $\boldsymbol{k}\alpha$. The derivation of (11) was based on the assumption that the coupling of the $c_{\boldsymbol{k}\alpha}(\boldsymbol{G},z)$ for different $\boldsymbol{G}$ via $v(\boldsymbol{G}\neq\boldsymbol{0},z)$ can be ignored for large z. Inclusion of this coupling leads to contributions vanishing like $v(\boldsymbol{G},z)c_{\boldsymbol{k}\alpha}(\boldsymbol{0},z)$ in all $c_{\boldsymbol{k}\alpha}(\boldsymbol{G},z)$ with $\boldsymbol{G}\neq\boldsymbol{0}$. However, since $v(\boldsymbol{G}\neq\boldsymbol{0},z)$ decays faster than $1/z$, these contributions are irrelevant for the present discussion.

On the basis of the exponential decay of the KS states into the vacuum, it has been demonstrated [40] that the EXX energy density behaves as

$$e_{\rm x}(\boldsymbol{r}) \xrightarrow{z\gg L} -\frac{n(\boldsymbol{r})}{2z}. \tag{13}$$

As a consequence, $v_{\rm Slater}$ falls off as $-1/z$, just like the exact $v_{\rm x}$ [47],

$$v_{\rm Slater}(\boldsymbol{r}) \xrightarrow{z\gg L} -\frac{1}{z}. \tag{14}$$

Note that this asymptotic behavior is in line with the normalization of the total $v_{\rm s}$ expressed in Eq. (10). An explicit normalization of $v_{\rm Slater}$ is not necessary.

The discussion of the asymptotic behavior of $v_{\rm shift}$ is more intricate. Focusing first on the density in the denominator of (8), insertion of the Fourier expansion (2) into (3) yields

$$n(\boldsymbol{r}) = 2\sum_{\boldsymbol{G}} e^{i\boldsymbol{G}\cdot\boldsymbol{r}_\parallel} \int_{\rm 1BZ} \frac{d^2k}{(2\pi)^2} \sum_\alpha \Theta_{\boldsymbol{k}\alpha} \times \sum_{\boldsymbol{G}'} c^*_{\boldsymbol{k}\alpha}(\boldsymbol{G}',z)\, c_{\boldsymbol{k}\alpha}(\boldsymbol{G}'+\boldsymbol{G},z)\,. \tag{15}$$

Asymptotically, the density is dominated by the Fourier coefficients $c_{\boldsymbol{k}\alpha}$ with $\boldsymbol{G}=\boldsymbol{0}$ since these coefficients decay most slowly [47],

$$n(\boldsymbol{r}) \xrightarrow{z\gg L} 2\int_{\rm 1BZ} \frac{d^2k}{(2\pi)^2} \sum_\alpha \Theta_{\boldsymbol{k}\alpha}\, |c_{\boldsymbol{k}\alpha}(\boldsymbol{0},z)|^2\,. \tag{16}$$

However, the expression in the numerator of (8) has exactly the same structure as $n(\boldsymbol{r})$, so that one finds

$$v_{\rm shift}(\boldsymbol{r}) \xrightarrow{z\gg L} \frac{\sum_\alpha \int_{\rm 1BZ} \frac{d^2k}{(2\pi)^2} \Theta_{\boldsymbol{k}\alpha}\Delta_{\boldsymbol{k}\alpha} |c_{\boldsymbol{k}\alpha}(\boldsymbol{0},z)|^2}{\sum_\alpha \int_{\rm 1BZ} \frac{d^2k}{(2\pi)^2} \Theta_{\boldsymbol{k}\alpha} |c_{\boldsymbol{k}\alpha}(\boldsymbol{0},z)|^2}. \tag{17}$$

In order to extract the behavior of v_{shift} for large z, the BZ integrations in (17) have to be performed, utilizing the asymptotic form of the Bloch coefficients, Eq. (11). Since the structures of the BZ integrals in the numerator and the denominator are identical, the BZ integration will be discussed for a generic integrand of this type in the next section.

III. BRILLOUIN ZONE INTEGRATION FOR $z \to \infty$

Consider the generic BZ integral with the asymptotic Bloch coefficients (11),

$$I = \int_{1\text{BZ}} \frac{d^2k}{(2\pi)^2}\, \Theta_{\boldsymbol{k}\alpha}\, \tilde{A}_{\boldsymbol{k}\alpha}\, |c_{\boldsymbol{k}\alpha}(\boldsymbol{0},z)|^2$$
$$= \int_{1\text{BZ}} \frac{d^2k}{(2\pi)^2}\, \Theta_{\boldsymbol{k}\alpha}\, A_{\boldsymbol{k}\alpha}\, z^{2u/\gamma_{\boldsymbol{k}\alpha}}\, e^{-2\gamma_{\boldsymbol{k}\alpha} z}. \tag{18}$$

Here $\gamma_{\boldsymbol{k}\alpha}$ abbreviates the exponent (12) at $\boldsymbol{G} = \boldsymbol{0}$,

$$\gamma_{\boldsymbol{k}\alpha} \equiv \gamma_{\boldsymbol{k}\alpha}(\boldsymbol{G} = \boldsymbol{0}) = [\boldsymbol{k}^2 - 2\epsilon_{\boldsymbol{k}\alpha}]^{1/2}, \tag{19}$$

and $A_{\boldsymbol{k}\alpha}$ is assumed to be twice differentiable with respect to $\boldsymbol{k}$ throughout the complete BZ. For large z the most weakly decaying contributions to the integral (18) are found in the vicinity of the lowest value of $\gamma_{\boldsymbol{k}\alpha}$ for all $\boldsymbol{k}$ for which $\Theta_{\boldsymbol{k}\alpha}$ is nonzero (the latter condition is, of course, relevant for only the highest occupied bands which may be partially filled). Several situations need to be distinguished.

A. Unique minimum of $\gamma_{\boldsymbol{k}\alpha}$ in the interior

We first consider the case where (i) there is a unique $\boldsymbol{k}$ point, in the following denoted by $\boldsymbol{q}$, for which $\gamma_{\boldsymbol{k}\alpha}$ has a global minimum (inside the BZ),

$$\frac{\partial \epsilon_{\boldsymbol{k}\alpha}}{\partial \boldsymbol{k}}(\boldsymbol{q}) = \boldsymbol{q}, \tag{20}$$

and (ii) the band α for which (18) is to be calculated is occupied in a complete neighborhood of $\boldsymbol{q}$. This situation is met quite often, as illustrated in Fig. 1 for graphene and two Si(111) slabs of different thicknesses. As Fig. 1 demonstrates, $\boldsymbol{q}$ is typically the Γ point. This statement is not only true for a single band but also applies if the minimum $\gamma_{\boldsymbol{k}\alpha}$ of all occupied bands is considered, as is done in Fig. 1: while the occupied states with the highest $\epsilon_{\boldsymbol{k}\alpha}$ are often found at nonzero $\boldsymbol{k}$, the quantity $\boldsymbol{k}^2 - 2\epsilon_{\boldsymbol{k}\alpha}$ is nevertheless minimized for $\boldsymbol{k} = \boldsymbol{0}$ and lower $\epsilon_{\boldsymbol{k}\alpha}$.

For large z the exponential function $e^{-2\gamma_{\boldsymbol{k}\alpha} z}$ varies much more rapidly with $\boldsymbol{k}$ than all other components of the integrand in (18). It has its peak at $\boldsymbol{k} = \boldsymbol{q}$, and the same is true for $z^{2u/\gamma_{\boldsymbol{k}\alpha}}$. As long as $A_{\boldsymbol{k}\alpha}$ is differentiable in a neighborhood of $\boldsymbol{q}$, one can thus utilize a Taylor expansion of $\gamma_{\boldsymbol{k}\alpha}$,

$$\gamma_{\boldsymbol{k}\alpha} = \gamma_{\boldsymbol{q}\alpha} + \tfrac{1}{2}(\boldsymbol{k} - \boldsymbol{q})\Gamma_{\boldsymbol{q}\alpha}(\boldsymbol{k} - \boldsymbol{q}) + \cdots, \tag{21}$$

$$\Gamma_{\boldsymbol{q}\alpha} = \frac{\partial^2 \gamma_{\boldsymbol{k}\alpha}}{\partial \boldsymbol{k} \partial \boldsymbol{k}}(\boldsymbol{q}), \tag{22}$$

to extract the leading term of the integral (18) for large z [48]. The contributions from the regions of the BZ for which (21) is not valid are exponentially suppressed compared to those from the vicinity of $\boldsymbol{q}$, irrespective of whether the left- or the right-hand side of (21) is used in $e^{-2\gamma_{\boldsymbol{k}\alpha} z}$.

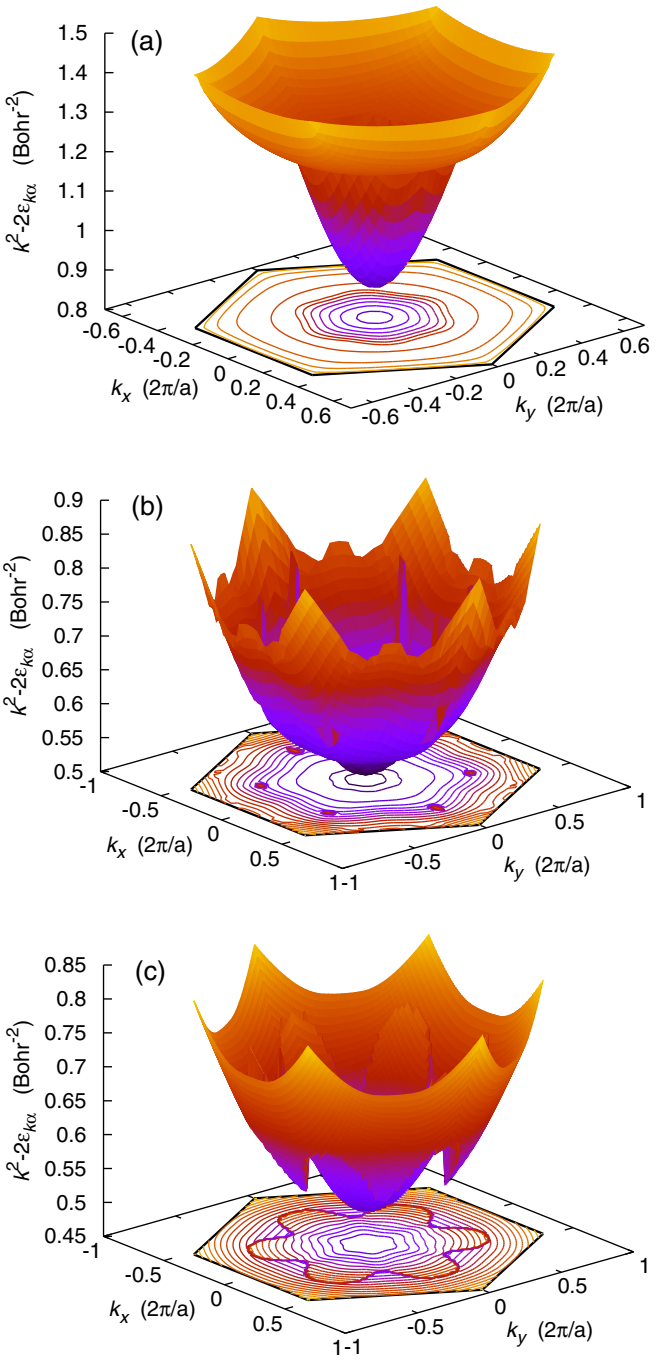

FIG. 1. Exponent $\boldsymbol{k}^2 - 2\epsilon_{\boldsymbol{k}\alpha}$ for the highest occupied band at $\boldsymbol{k}$ throughout the first Brillouin zone (indicated by black lines) for (a) graphene, (b) a 6-layer Si(111) slab, and (c) an 18-layer Si(111) slab. The band energies have been obtained by EXX calculations, utilizing the KLI approximation. The discontinuities in the case of the Si(111) slabs result from different bands being the highest occupied one for different $\boldsymbol{k}$.

Moreover, the second-order Taylor expansion can also be employed for $z^{2u/\gamma_{\boldsymbol{k}\alpha}}$. A straightforward Taylor expansion of the complete function $z^{2u/\gamma_{\boldsymbol{k}\alpha}}$,

$$z^{2u/\gamma_{\boldsymbol{k}\alpha}} = z^{2u/\gamma_{\boldsymbol{q}\alpha}} \left[1 - \frac{u}{\gamma_{\boldsymbol{q}\alpha}^2} \ln(z)(\boldsymbol{k} - \boldsymbol{q})\Gamma_{\boldsymbol{q}\alpha}(\boldsymbol{k} - \boldsymbol{q})\right],$$

however, does not satisfy the rigorous requirement

$$0 < z^{2u/\gamma_{k\alpha}}$$

for all $\boldsymbol{k}$. For that reason the expansion (21) is more conveniently applied in the exponent of $z^{2u/\gamma_{k\alpha}}$, which amounts to a partial resummation of the Taylor expansion of the complete function. This resummation of terms proportional to $[\ln(z)/z]^n$ is legitimate and appropriate as long as (i) one has

$$z^{2u/\gamma_{k\alpha}} \approx z^{2u/\gamma_{q\alpha}}\, z^{-(\boldsymbol{k}-\boldsymbol{q})\Gamma_{q\alpha}(\boldsymbol{k}-\boldsymbol{q})u/\gamma_{q\alpha}^2}$$

in the relevant part of the integration region and (ii) the resummation does not lead to any convergence problems with the $\boldsymbol{k}$ integral in (18).

In order to implement the expansion (21) one thus rewrites (18) as

$$I = \int_{1\mathrm{BZ}} \frac{d^2k}{(2\pi)^2}\, \Theta_{k\alpha}\, A_{k\alpha}\, e^{-2\gamma_{k\alpha}z + 2u\ln(z)/\gamma_{k\alpha}}$$

and subsequently applies the expansion in the exponent,

$$I \xrightarrow{z\gg L} z^{2u/\gamma_{q\alpha}}\, e^{-2\gamma_{q\alpha}z} \int_{1\mathrm{BZ}} \frac{d^2k}{(2\pi)^2}\, \Theta_{k\alpha}\, A_{k\alpha} \times e^{-(\boldsymbol{k}-\boldsymbol{q})\Gamma_{q\alpha}(\boldsymbol{k}-\boldsymbol{q})[z+u\ln(z)/\gamma_{q\alpha}^2]}. \tag{23}$$

The limited variation of $A_{k\alpha}$ over the small region around $\boldsymbol{q}$ for which the exponential function is non-negligible for large z allows us to approximate $A_{k\alpha}$ by its Taylor expansion around $\boldsymbol{q}$,

$$A_{k\alpha} = A_{q\alpha} + \mathbf{B}_{q\alpha}\cdot(\boldsymbol{k}-\boldsymbol{q}) + \tfrac{1}{2}(\boldsymbol{k}-\boldsymbol{q})\mathbf{C}_{q\alpha}(\boldsymbol{k}-\boldsymbol{q}) + \cdots, \tag{24}$$

$$\mathbf{B}_{q\alpha} = \frac{\partial A_{k\alpha}}{\partial \boldsymbol{k}}(\boldsymbol{q}), \tag{25}$$

$$\mathbf{C}_{q\alpha} = \frac{\partial^2 A_{k\alpha}}{\partial \boldsymbol{k}\partial \boldsymbol{k}}(\boldsymbol{q}). \tag{26}$$

In fact, as long as (i) $A_{q\alpha}$ is nonzero, (ii) z is sufficiently large, and (iii) one is interested only in the asymptotically leading term, $A_{k\alpha}$ can simply be approximated by its value at $\boldsymbol{k} = \boldsymbol{q}$,

$$I \xrightarrow{z\gg L} A_{q\alpha}\, z^{2u/\gamma_{q\alpha}}\, e^{-2\gamma_{q\alpha}z} \int_{1\mathrm{BZ}} \frac{d^2k}{(2\pi)^2}\, \Theta_{k\alpha} \times e^{-(\boldsymbol{k}-\boldsymbol{q})\Gamma_{q\alpha}(\boldsymbol{k}-\boldsymbol{q})[z+u\ln(z)/\gamma_{q\alpha}^2]}. \tag{27}$$

Similarly, since a complete neighborhood of $\boldsymbol{q}$ is assumed to be occupied and this neighborhood completely dominates (27) for large z, the occupation factor can be replaced by 1. Due to the rapid exponential decay for large z one can finally extend the $\boldsymbol{k}$ integration to the complete $\boldsymbol{k}$ space without loss of accuracy,

$$I \xrightarrow{z\gg L} A_{q\alpha}\, z^{2u/\gamma_{q\alpha}}\, e^{-2\gamma_{q\alpha}z} \int \frac{d^2k}{(2\pi)^2}\, e^{-\boldsymbol{k}\Gamma_{q\alpha}\boldsymbol{k}[z+u\ln(z)/\gamma_{q\alpha}^2]} = \frac{z^{2u/\gamma_{q\alpha}}\, e^{-2\gamma_{q\alpha}z}}{\left[z+u\ln(z)/\gamma_{q\alpha}^2\right]}\,\bar{A}, \tag{28}$$

$$\bar{A} = \frac{1}{4\pi}\, A_{q\alpha}\, [\det(\Gamma_{q\alpha})]^{-1/2} \tag{29}$$

(note that the 2×2 matrix $\Gamma_{q\alpha}$ is positive definite by construction).

The situation is slightly different if $A_{q\alpha} = 0$. Since

$$\mathbf{B}_{q\alpha}\cdot\int \frac{d^2k}{(2\pi)^2}\, \boldsymbol{k}\, e^{-\boldsymbol{k}\Gamma_{q\alpha}\boldsymbol{k}[z+u\ln(z)/\gamma_{q\alpha}^2]} = 0, \tag{30}$$

the first-order term in the expansion (24) does not contribute. Consequently, the second-order term gives the first nonvanishing contribution,

$$I \xrightarrow{z\gg L} \frac{1}{2}\, z^{2u/\gamma_{q\alpha}}\, e^{-2\gamma_{q\alpha}z} \int \frac{d^2k}{(2\pi)^2}\, \boldsymbol{k}\mathbf{C}_{q\alpha}\boldsymbol{k}\, e^{-\boldsymbol{k}\Gamma_{q\alpha}\boldsymbol{k}[z+u\ln(z)/\gamma_{q\alpha}^2]} = \frac{z^{2u/\gamma_{q\alpha}}\, e^{-2\gamma_{q\alpha}z}}{\left[z+u\ln(z)/\gamma_{q\alpha}^2\right]^2}\,\bar{C}, \tag{31}$$

$$\bar{C} = \frac{1}{16\pi}\,\mathrm{tr}\big(\mathbf{C}_{q\alpha}\Gamma_{q\alpha}^{-1}\big)[\det(\Gamma_{q\alpha})]^{-1/2}. \tag{32}$$

The expansion (24) has to be extended to fourth order if not only $A_{q\alpha}$ but also $\mathbf{C}_{q\alpha}$ vanishes. The evaluation of the BZ integral can, however, still follow the same line as used for the derivation of (31). It is obvious that the result is proportional to $[z+u\ln(z)/\gamma_{q\alpha}^2]^{-3}$ in this case.

B. Finite number of minima of $\gamma_{k\alpha}$ in the interior

Next, we extend the above discussion to the case when there is a finite number of points $\boldsymbol{q}_i$ for which $\gamma_{k\alpha}$ has minima with the same value,

$$\frac{\partial \epsilon_{k\alpha}}{\partial \boldsymbol{k}}(\boldsymbol{q}_i) = \boldsymbol{q}_i, \quad i = 1,\ldots m, \tag{33}$$

$$\gamma_{q_i\alpha} = \gamma_{q_j\alpha} \equiv \gamma_{q\alpha}, \quad i,j = 1,\ldots m, \tag{34}$$

while the band α is still assumed to be occupied in complete neighborhoods of these $\boldsymbol{q}_i$. In this situation the BZ can be split into m disjoint, simply connected cells V_i, with V_i containing $\boldsymbol{q}_i$ as an interior point,

$$I = \sum_{i=1}^{m} I_i, \tag{35}$$

$$I_i = \int_{V_i} \frac{d^2k}{(2\pi)^2}\, \Theta_{k\alpha}\, A_{k\alpha}\, z^{2u/\gamma_{k\alpha}}\, e^{-2\gamma_{k\alpha}z}. \tag{36}$$

Since all $\boldsymbol{q}_i$ are distinct, a precise definition of the cell boundaries is not necessary at this point (with the understanding that $\boldsymbol{q}_i$ is somewhere close to the "center" of V_i). Each individual I_i can be handled in the same fashion as the integral over the complete BZ in the case of a unique minimum since only the immediate neighborhood of $\boldsymbol{q}_i$ is relevant for large z. The results of Sec. III A can therefore be directly employed for all I_i. Noting that, due to (34), the z dependences emerging from all I_i are identical, one finds the same asymptotic behavior as in (28), with the coefficient (29) replaced by

$$\bar{A} = \frac{1}{4\pi}\sum_{i=1}^{m} A_{q_i\alpha}\, [\det(\Gamma_{q_i\alpha})]^{-1/2}, \tag{37}$$

and similarly for (31).

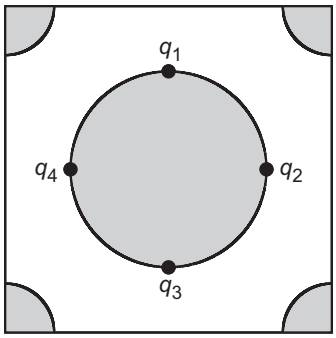

FIG. 2. Integration region (shaded area) for partially filled band with degenerate minima of $\gamma_{k\alpha}$ at the boundary of the integration region.

C. Finite number of minima of $\gamma_{k\alpha}$ in the interior for several bands

When comparing the asymptotic behavior of different bands, it is clear from Eqs. (18), (28), and (31) that the band with the minimum $\gamma_{q\alpha}$ ultimately dominates for large z. If the minimum $\gamma_{q\alpha}$ results from only a single band, quantities involving sums over bands can be evaluated from Eqs. (28) and (31) (or their extensions to several $\boldsymbol{q}_i$) for this particular band. If the same minimum value $\gamma_{q\alpha}$ is found for more than one band, one can use the argument of Sec. III B to combine sums over these bands into one expression. Once again, the asymptotics of all bands is dominated by the same value $\gamma_{q\alpha}$, so that one obtains the z dependences of Eqs. (28) and (31) (or mixtures of both) with the coefficients $\bar{A}$ and $\bar{C}$ now involving sums over several bands and $\boldsymbol{k}$ points.

D. Lowest value of $\gamma_{k\alpha}$ at the boundary

We finally consider the case when the lowest value of $\gamma_{k\alpha}$ in the integration region is found right at the boundary of this region. This situation can result either from $\boldsymbol{q}$ being located at the boundary of the BZ or from the band passing through the Fermi surface. A sketch of the latter situation (with four degenerate minima) is given in Fig. 2. A more realistic picture is provided in Fig. 3, which shows $\gamma^2_{k\alpha}$ for a seven-layer Al(100) slab. Figure 3(a) demonstrates that the lowest $\gamma_{k\alpha}$ values for different $\boldsymbol{k}$ values originate from different bands: in this plot the boundaries between the associated regions of $\boldsymbol{k}$ space (at which $\gamma_{k\alpha}$ is discontinuous) are indicated as white contours. At the boundaries particular bands cross the Fermi level; that is, the boundaries correspond to the 2D Fermi surface. For all points $\boldsymbol{k}_\mathrm{b}$ on a boundary one thus has

$$\epsilon_{\boldsymbol{k}_\mathrm{b}\alpha} = \epsilon_\mathrm{F}. \tag{38}$$

Assuming $\boldsymbol{k}_\mathrm{b}(s)$ to be a parameter representation of a contour, the tangent to the boundary satisfies the relation

$$\frac{d\boldsymbol{k}_\mathrm{b}}{ds}(s) \cdot \frac{\partial \epsilon_{\boldsymbol{k}\alpha}}{\partial \boldsymbol{k}}[\boldsymbol{k}_\mathrm{b}(s)] = 0. \tag{39}$$

Figure 3(b) shows the most important region with the minimum values of $\gamma_{k\alpha}$ on an enlarged scale. One clearly recognizes that the lowest value is obtained right at a boundary between two bands, while the exponent is rather flat in the

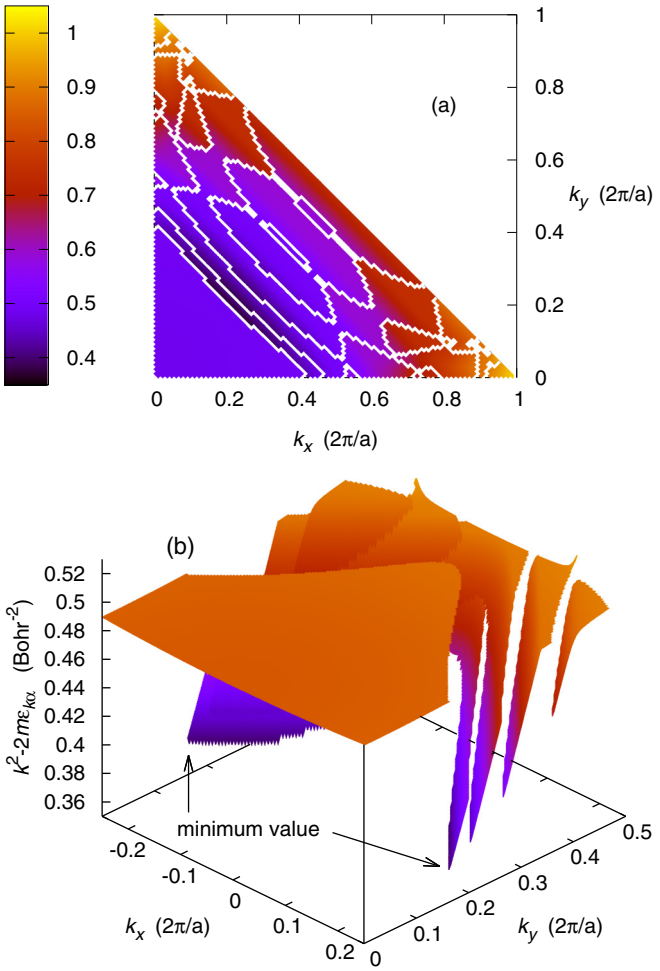

FIG. 3. Exponent $\boldsymbol{k}^2 - 2\epsilon_{k\alpha}$ for the highest occupied band at $\boldsymbol{k}$ for a seven-layer Al(100) slab: (a) projection on the k_x-k_y plane in one quarter of the first Brillouin zone and (b) 3D representation of the most relevant region on an enlarged scale. Arrows point at the $\boldsymbol{k}$ values for which $\boldsymbol{k}^2 - 2\epsilon_{k\alpha}$ assumes its lowest value (the minima are somewhat masked by the finite resolution of the plot). (b) explicitly demonstrates the discontinuity of $\boldsymbol{k}^2 - 2\epsilon_{k\alpha}$. The band energies have been obtained with an EXX calculation, utilizing the KLI approximation.

neighborhood of the Γ point. If the point on the boundary at which $\gamma_{k\alpha}$ assumes its minimum value is denoted by $\boldsymbol{q} = \boldsymbol{k}_\mathrm{b}(s_q)$, the gradient of $\gamma_{k\alpha}$ at $\boldsymbol{q}$ has to be orthogonal to the tangent along the contour at this point [49],

$$\frac{d\boldsymbol{k}_\mathrm{b}}{ds}(s_q) \cdot \mathbf{D}_{q\alpha} = 0, \tag{40}$$

$$\mathbf{D}_{q\alpha} = \frac{\partial \gamma_{k\alpha}}{\partial \boldsymbol{k}}(\boldsymbol{q}). \tag{41}$$

Restricting the discussion to a single point $\boldsymbol{q}$, one can basically follow the arguments in Sec. III A. However, since the lowest value of $\gamma_{k\alpha}$ within the integration region, at least in general, no longer coincides with a minimum of $\gamma_{k\alpha}$ in the complete BZ, the first-order term of the expansion (21) does not vanish at $\boldsymbol{q}$,

$$\gamma_{k\alpha} = \gamma_{q\alpha} + \mathbf{D}_{q\alpha} \cdot (\boldsymbol{k} - \boldsymbol{q}) + \tfrac{1}{2}(\boldsymbol{k} - \boldsymbol{q})\Gamma_{q\alpha}(\boldsymbol{k} - \boldsymbol{q}) + \cdots . \tag{42}$$

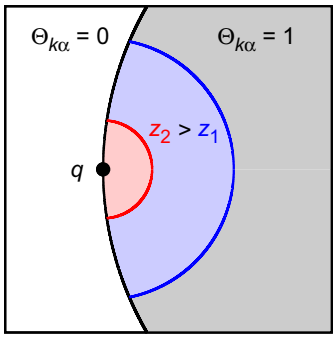

FIG. 4. Complete integration region (gray shaded area) of a partially filled band with a global minimum of $\gamma_{k\alpha}$ at $\boldsymbol{q}$ versus the relevant integration region for large z: the blue shaded region relevant for z_2 gives the same percentage contribution to the total integral as the red shaded region relevant for $z_1 < z_2$.

In addition, $\Gamma_{\boldsymbol{q}\alpha}$ no longer need to be positive definite. The only remaining requirement is that there is a minimum in the direction along the boundary,

$$\frac{d\boldsymbol{k}_\mathrm{b}}{ds}(s_q)\Gamma_{\boldsymbol{q}\alpha}\frac{d\boldsymbol{k}_\mathrm{b}}{ds}(s_q) > 0. \tag{43}$$

Focusing on the situation $\mathbf{D}_{\boldsymbol{q}\alpha} \neq \mathbf{0}$ first (the case $\mathbf{D}_{\boldsymbol{q}\alpha} = 0$ is dealt with below), Eq. (27) has to be modified to

$$I \xrightarrow{z\gg L} A_{\boldsymbol{q}\alpha}\, z^{2u/\gamma_{\boldsymbol{q}\alpha}}\, e^{-2\gamma_{\boldsymbol{q}\alpha}z} \int_{1\mathrm{BZ}} \frac{d^2k}{(2\pi)^2}\,\Theta_{\boldsymbol{k}\alpha} \times e^{-[2\mathbf{D}_{\boldsymbol{q}\alpha}\cdot(\boldsymbol{k}-\boldsymbol{q})+(\boldsymbol{k}-\boldsymbol{q})\Gamma_{\boldsymbol{q}\alpha}(\boldsymbol{k}-\boldsymbol{q})]z}, \tag{44}$$

where corrections of the order $\ln(z)/z$ have been neglected in order to simplify the discussion.

One next has to account for the fact that part of the BZ (or, more generally, the cell around $\boldsymbol{q}$) does not belong to the integration region, as the occupation function vanishes there. With increasing z the relevant integration area around $\boldsymbol{q}$ shrinks further and further, so that the boundary between $\Theta_{k\alpha} = 1$ and $\Theta_{\boldsymbol{k}\alpha} = 0$ inside this area ultimately becomes the straight line defined by

$$\boldsymbol{q} + \frac{d\boldsymbol{k}_\mathrm{b}}{ds}(s_q)\, s, \quad s \in \mathbb{R} \tag{45}$$

(since the curvature of the boundary is independent of z and fixed). An illustration of this scaling effect is given in Fig. 4. When extending the relevant integration region to the complete 2D $\boldsymbol{k}$ space, one ends up with an integration over half of the k_x-k_y plane, with $\boldsymbol{q}$ being located on the straight line between the two halves. As in the unrestricted situation, one can subsequently shift the origin of the $\boldsymbol{k}$ integration to the point $\boldsymbol{q}$,

$$I \xrightarrow{z\gg L} A_{\boldsymbol{q}\alpha}\, z^{2u/\gamma_{\boldsymbol{q}\alpha}}\, e^{-2\gamma_{\boldsymbol{q}\alpha}z} \int_H \frac{d^2k}{(2\pi)^2}\, e^{-[2\mathbf{D}_{\boldsymbol{q}\alpha}\cdot\boldsymbol{k}+\boldsymbol{k}\Gamma_{\boldsymbol{q}\alpha}\boldsymbol{k}]z}. \tag{46}$$

Here H implements the restriction of the integration to that half of the 2D $\boldsymbol{k}$ space for which

$$\mathbf{D}_{\boldsymbol{q}\alpha}\cdot\boldsymbol{k} > 0. \tag{47}$$

The straight line separating the integration region from the exterior region now goes through the shifted origin.

The behavior of the exponent in (46) is dominated by the first-order term in the direction of $\mathbf{D}_{\boldsymbol{q}\alpha}$ (at least close to the minimum at $\boldsymbol{q}$) and by the second-order term in the orthogonal direction parallel to the boundary line. One thus chooses the orientation of the coordinate system for the $\boldsymbol{k}$ integration such that the coordinate k_1 is parallel to $\mathbf{D}_{\boldsymbol{q}\alpha}$ and the coordinate k_2 is parallel to the boundary line,

$$I \xrightarrow{z\gg L} A_{\boldsymbol{q}\alpha}\, z^{2u/\gamma_{\boldsymbol{q}\alpha}}\, e^{-2\gamma_{\boldsymbol{q}\alpha}z} \int_0^\infty \frac{dk_1}{2\pi} \int_{-\infty}^\infty \frac{dk_2}{2\pi} \times e^{-[2|\mathbf{D}_{\boldsymbol{q}\alpha}|k_1+\boldsymbol{n}_\perp\Gamma_{\boldsymbol{q}\alpha}\boldsymbol{n}_\perp k_2^2]z}, \tag{48}$$

where $\boldsymbol{n}_\perp$ denotes a unit vector in the direction of the boundary line. The asymptotically leading term is thus given by

$$I \xrightarrow{z\gg L} \frac{A_{\boldsymbol{q}\alpha}\, z^{2u/\gamma_{\boldsymbol{q}\alpha}}\, e^{-2\gamma_{\boldsymbol{q}\alpha}z}}{8\pi^{3/2}|\mathbf{D}_{\boldsymbol{q}\alpha}|\,[\boldsymbol{n}_\perp\Gamma_{\boldsymbol{q}\alpha}\boldsymbol{n}_\perp]^{1/2}\, z^{3/2}}. \tag{49}$$

Comparing this equation to the result (28), one observes an additional factor of $\sqrt{z}$ in the denominator.

If $A_{\boldsymbol{q}\alpha} = 0$, the asymptotically leading contribution emerges from the first-order term of the Taylor expansion (24),

$$I \xrightarrow{z\gg L} z^{2u/\gamma_{\boldsymbol{q}\alpha}}\, e^{-2\gamma_{\boldsymbol{q}\alpha}z} \int_H \frac{d^2k}{(2\pi)^2}\, \mathbf{B}_{\boldsymbol{q}\alpha}\cdot\boldsymbol{k} \times e^{-[2\mathbf{D}_{\boldsymbol{q}\alpha}\cdot\boldsymbol{k}+\boldsymbol{k}\Gamma_{\boldsymbol{q}\alpha}\boldsymbol{k}]z}$$

[since Eq. (30) relies on the $\boldsymbol{k}$ integration extending over the complete 2D $\boldsymbol{k}$ space]. Proceeding as before, one finds

$$I \xrightarrow{z\gg L} \frac{\mathbf{B}_{\boldsymbol{q}\alpha}\cdot\mathbf{D}_{\boldsymbol{q}\alpha}\, z^{2u/\gamma_{\boldsymbol{q}\alpha}}\, e^{-2\gamma_{\boldsymbol{q}\alpha}z}}{16\pi^{3/2}|\mathbf{D}_{\boldsymbol{q}\alpha}|^3\,[\boldsymbol{n}_\perp\Gamma_{\boldsymbol{q}\alpha}\boldsymbol{n}_\perp]^{1/2}\, z^{5/2}}. \tag{50}$$

It is obvious from the discussion in Secs. III B and III C that the results (49) and (50) can be extended to the case with several points $\boldsymbol{q}_i$.

The (less likely) case that $\mathbf{D}_{\boldsymbol{q}\alpha} = \mathbf{0}$ although $\boldsymbol{q}$ is a point on a boundary of the integration region remains to be discussed. In this situation $\Gamma_{\boldsymbol{q}\alpha}$ is again positive definite. Starting from (27) and proceeding as for the derivation of (46), one obtains

$$I \xrightarrow{z\gg L} A_{\boldsymbol{q}\alpha}\, z^{2u/\gamma_{\boldsymbol{q}\alpha}}\, e^{-2\gamma_{\boldsymbol{q}\alpha}z} \times \int_H \frac{d^2k}{(2\pi)^2}\, e^{-\boldsymbol{k}\Gamma_{\boldsymbol{q}\alpha}\boldsymbol{k}[z+u\ln(z)/\gamma_{\boldsymbol{q}\alpha}^2]}. \tag{51}$$

As in Eq. (46), H is that half of 2D $\boldsymbol{k}$ space which emerges from the condition $\Theta_{\boldsymbol{k}\alpha} > 1$; that is, H is defined by the straight line (45). One can now scale both components of $\boldsymbol{k}$ by the (large) positive factor $[z + u\ln(z)/\gamma_{\boldsymbol{q}\alpha}^2]^{1/2}$,

$$\boldsymbol{k}' = \left[z + u\ln(z)/\gamma_{\boldsymbol{q}\alpha}^2\right]^{1/2}\boldsymbol{k}, \tag{52}$$

to arrive at

$$I \xrightarrow{z\gg L} \frac{A_{\boldsymbol{q}\alpha}\, z^{2u/\gamma_{\boldsymbol{q}\alpha}}\, e^{-2\gamma_{\boldsymbol{q}\alpha}z}}{\left[z + u\ln(z)/\gamma_{\boldsymbol{q}\alpha}^2\right]} \int_H \frac{d^2k'}{(2\pi)^2}\, e^{-\boldsymbol{k}'\Gamma_{\boldsymbol{q}\alpha}\boldsymbol{k}'}. \tag{53}$$

This equation uses the fact that the integration region of the scaled variable $\boldsymbol{k}'$ is exactly the same as that for $\boldsymbol{k}$ since H is

bounded by a straight line through the origin and the scaling is homogeneous. One thus obtains exactly the same asymptotic z dependence as in (28), with $\bar{A}$ now given by

$$\bar{A} = A_{\boldsymbol{q}\alpha} \int_H \frac{d^2k'}{(2\pi)^2}\, e^{-\boldsymbol{k}'\Gamma_{\boldsymbol{q}\alpha}\boldsymbol{k}'}. \tag{54}$$

A z dependence different from Eq. (31) is, however, found in the case $A_{\boldsymbol{q}\alpha} = 0$. As in the case of Eq. (50), the leading contribution emerges from the first-order term of the Taylor expansion (24),

$$I \xrightarrow{z\gg L} \frac{z^{2u/\gamma_{\boldsymbol{q}\alpha}}\, e^{-2\gamma_{\boldsymbol{q}\alpha}z}}{\left[z + u\ln(z)/\gamma_{\boldsymbol{q}\alpha}^2\right]^{3/2}}\, \bar{B}, \tag{55}$$

$$\bar{B} = \int_H \frac{d^2k'}{(2\pi)^2}\, \mathbf{B}_{\boldsymbol{q}\alpha}\cdot\boldsymbol{k}'\, e^{-\boldsymbol{k}'\Gamma_{\boldsymbol{q}\alpha}\boldsymbol{k}'}. \tag{56}$$

IV. ASYMPTOTIC BEHAVIOR OF THE ORBITAL-SHIFT POTENTIAL

To leading order, the asymptotic behavior of both the numerator and the denominator on the right-hand side of Eq. (17) is controlled by the vicinity of the $\boldsymbol{k}$ point(s) for which the exponent $\gamma_{\boldsymbol{k}\alpha}(\boldsymbol{G}=\boldsymbol{0})$ of Eq. (11) assumes its minimum value in the integration region. Depending on the shape of $\gamma_{\boldsymbol{k}\alpha}(\boldsymbol{G}=\boldsymbol{0})$, one arrives at Eqs. (28) and (31) or their counterparts for more complicated situations. If, for the relevant band(s) α, both $\Delta_{\boldsymbol{k}\alpha}$ and $f_{\boldsymbol{k}\alpha}(\boldsymbol{G}=\boldsymbol{0})$ are nonzero at the $\boldsymbol{k}$ point(s) with the minimum exponent, the numerator and the denominator in Eq. (17) exhibit the same z dependence, so that v_{shift} asymptotically approaches a nonzero constant.

However, proper normalization of the total KS potential, i.e., Eq. (10), requires

$$v_{\text{shift}}(\boldsymbol{r}) \xrightarrow{z\to\infty} 0, \tag{57}$$

since all other components of v_{s} and v_{Slater} also vanish in this limit. Restricting the discussion first to the simplest case in which the lowest value of $\gamma_{\boldsymbol{k}\alpha}(\boldsymbol{G}=\boldsymbol{0})$ is found for only a single band α at a single $\boldsymbol{k}$ point $\boldsymbol{q}$, the normalization (57) can be implemented by choosing

$$\Delta_{\boldsymbol{q}\alpha} = 0. \tag{58}$$

The expression on the right-hand side of (17) can then be evaluated further by the use of Eqs. (28) and (31),

$$v_{\text{shift}}(\boldsymbol{r}) \xrightarrow{z\gg L} \frac{\bar{C}}{\bar{A}\left[z + u\ln(z)/\gamma_{\boldsymbol{q}\alpha}^2\right]}, \tag{59}$$

with $\bar{A}$ and $\bar{C}$ defined by Eqs. (29) and (32), respectively. As a result one observes a $1/z$ decay of v_{shift}.

A $1/z$ dependence is also obtained in most other situations, in particular, if one has several degenerate states with the same $\gamma_{\boldsymbol{q}\alpha}$ or different $\boldsymbol{k}$ points which yield the same exponent (due to some symmetry). Also for metals, for which the minimum value of $\gamma_{\boldsymbol{k}\alpha}$ is typically found at $\boldsymbol{k}$ points corresponding to the Fermi surface, the ratio of (49) and (50) leads to a $1/z$ decay. Even if $f_{\boldsymbol{k}\alpha}(\boldsymbol{G}=\boldsymbol{0})$ vanishes, the same behavior is obtained: in this case the numerator in (17) is determined by (31) (or its counterparts), and the denominator in (17) is controlled by the fourth-order term of the Taylor expansion (24), so that the ratio is again proportional to $[z + u\ln(z)/\gamma_{\boldsymbol{q}\alpha}^2]^{-1}$. The normalization (57) can thus be ensured by choosing $\Delta_{\boldsymbol{k}\alpha}$ to vanish for the state(s) which dominate the density (16) for $z\to\infty$.

When the result (59) is combined with the asymptotic behavior of the Slater potential, Eq. (14), the total $v_{\text{x}}^{\text{KLI}}$,

$$v_{\text{x}}^{\text{KLI}}(\boldsymbol{r}) \xrightarrow{z\gg L} -\frac{1-u_{\text{s}}}{z}, \tag{60}$$

is found to deviate from the $-1/z$ dependence of the exact v_{x} [50]. It remains to be seen how large u_{s} is in practice. Its value depends on the Fourier amplitudes of the asymptotically leading states, their band energies, and their EXX energy densities, as well as the gradients of these quantities (via $\bar{A}$ and $\bar{C}$ or the corresponding coefficients for the more complicated situations). One could thus expect quite different values for different classes of slabs.

V. CONCLUDING REMARKS

Somewhat surprisingly, the behavior of the KLI approximation to the exact exchange potential far outside the surface of a slab is not completely determined by its Slater component. While the Slater potential shows the expected $-1/z$ decay [40], the second component of the KLI potential, the orbital-shift term, in general also falls off no faster than $1/z$. This conclusion is based on an analytical evaluation of the BZ integrals involved for several classes of band structures. Only weak assumptions about the differentiability of the band energies and Bloch amplitudes are required to perform the BZ integrations. These assumptions are well justified for many slabs, in particular for such prominent cases as graphene and Si(111) slabs.

The analytical BZ integration relies on a second-order Taylor expansion of the $\boldsymbol{k}$-dependent exponent controlling the exponential decay of the states $\gamma_{\boldsymbol{k}\alpha}$ about its minimum at some point $\boldsymbol{q}$,

$$e^{-2\gamma_{\boldsymbol{k}\alpha}z} \approx e^{-2\gamma_{\boldsymbol{q}\alpha}z}\, e^{-(\boldsymbol{k}-\boldsymbol{q})\Gamma_{\boldsymbol{q}\alpha}(\boldsymbol{k}-\boldsymbol{q})z}$$

(in the simplest situation, to which the discussion is restricted at this point). This expansion is based on the fact that for sufficiently large z only the immediate vicinity of the point $\boldsymbol{q}$ contributes sizably to the BZ integrals. The z values required for this to be the case depend on the shape of $\gamma_{\boldsymbol{k}\alpha}$. If $\gamma_{\boldsymbol{k}\alpha}$ has a very pronounced minimum, the factor $e^{-2\gamma_{\boldsymbol{k}\alpha}z}$ falls off rapidly with increasing $|\boldsymbol{k}-\boldsymbol{q}|$. On the other hand, in the case of a shallow minimum it needs extremely large z values to reduce the relevant integration region enough that the approximation is legitimate. The scale of the variation of $\gamma_{\boldsymbol{k}\alpha}$ in the vicinity of $\boldsymbol{q}$ defines the scale of the z values which can be dealt with: if one requires

$$e^{-2\gamma_{\boldsymbol{k}\alpha}z} < s\, e^{-2\gamma_{\boldsymbol{q}\alpha}z}, \quad s \ll 1,$$

one finds

$$z > \frac{\ln(s)}{2(\gamma_{\boldsymbol{q}\alpha} - \gamma_{\boldsymbol{k}\alpha})}.$$

A rough estimate of the lower bound for z can thus be obtained from $\boldsymbol{k}$ points for which $|\boldsymbol{k}-\boldsymbol{q}|$ is a fraction of the extension of the BZ. For example, in the case of graphene (compare Fig. 1) one has $\gamma_{\boldsymbol{k}\alpha} - \gamma_{\boldsymbol{q}\alpha} \approx 0.04\,\text{bohr}^{-1}$ for $|\boldsymbol{k}-\boldsymbol{q}| \approx \pi/(4a)$. A suppression s of one order of magnitude then leads to $z > 27$ bohrs. For the six-layer Si(111) slab the much shallower

minimum already requires $z > 123$ bohrs for the same s and $|\boldsymbol{k} - \boldsymbol{q}|$. It seems worthwhile to emphasize that the competition between several bands with similar $\gamma_{k\alpha}$ might introduce an even larger lower bound on z.

ACKNOWLEDGMENT

The calculations for this work were performed on the computer cluster of the LOEWE Center for Scientific Computing of J. W. Goethe University Frankfurt am Main.

[1] P. Rinke, A. Qteish, J. Neugebauer, C. Freysoldt, and M. Scheffler, New J. Phys. **7**, 126 (2005).

[2] A. Qteish, A. I. Al-Sharif, M. Fuchs, M. Scheffler, S. Boeck, and J. Neugebauer, Comput. Phys. Commun. **169**, 28 (2005).

[3] P. Rinke, M. Scheffler, A. Qteish, M. Winkelnkemper, D. Bimberg, and J. Neugebauer, Appl. Phys. Lett. **89**, 161919 (2006).

[4] M. Grüning, A. Marini, and A. Rubio, J. Chem. Phys. **124**, 154108 (2006).

[5] P. Carrier, S. Rohra, and A. Görling, Phys. Rev. B **75**, 205126 (2007).

[6] J. Spencer and A. Alavi, Phys. Rev. B **77**, 193110 (2008).

[7] J. Harl and G. Kresse, Phys. Rev. B **77**, 045136 (2008).

[8] J. Harl and G. Kresse, Phys. Rev. Lett. **103**, 056401 (2009).

[9] E. Engel and R. N. Schmid, Phys. Rev. Lett. **103**, 036404 (2009).

[10] X. Wu, A. Selloni, and R. Car, Phys. Rev. B **79**, 085102 (2009).

[11] E. Engel, Phys. Rev. B **80**, 161205(R) (2009).

[12] J. Harl, L. Schimka, and G. Kresse, Phys. Rev. B **81**, 115126 (2010).

[13] M. Greiner, P. Carrier, and A. Görling, Phys. Rev. B **81**, 155119 (2010).

[14] E. J. Bylaska, K. Tsemekhman, S. B. Baden, J. H. Weare, and H. Jonsson, J. Comput. Chem. **32**, 54 (2011).

[15] M. Betzinger, C. Friedrich, S. Blügel, and A. Görling, Phys. Rev. B **83**, 045105 (2011).

[16] N. A. W. Holzwarth and X. Xu, Phys. Rev. B **84**, 113102 (2011).

[17] T. W. Hollins, S. J. Clark, K. Refson, and N. I. Gidopoulos, Phys. Rev. B **85**, 235126 (2012).

[18] M. Betzinger, C. Friedrich, A. Görling, and S. Blügel, Phys. Rev. B **85**, 245124 (2012).

[19] M. Betzinger, C. Friedrich, and S. Blügel, Phys. Rev. B **88**, 075130 (2013).

[20] H. Schulz and A. Görling, in *Frontiers and Challenges in Warm Dense Matter*, edited by F. Graziani, M. P. Desjarlais, R. Redmer, and S. B. Trickey, Lecture Notes in Computational Science and Engineering Vol. 96 (Springer, Berlin, 2014), p. 87.

[21] J. Klimes and G. Kresse, J. Chem. Phys. **140**, 054516 (2014).

[22] T. Fukazawa and H. Akai, J. Phys. Condens. Matter **27**, 115502 (2015).

[23] F. Tran, P. Blaha, M. Betzinger, and S. Blügel, Phys. Rev. B **94**, 165149 (2016).

[24] W. Zhu, L. Zhang, and S. B. Trickey, J. Chem. Phys. **145**, 224106 (2016).

[25] S. Kümmel and L. Kronik, Rev. Mod. Phys. **80**, 3 (2008).

[26] E. Engel and R. M. Dreizler, *Density Functional Theory: An Advanced Course* (Springer, Berlin, 2011).

[27] J. D. Talman and W. F. Shadwick, Phys. Rev. A **14**, 36 (1976).

[28] J. B. Krieger, Y. Li, and G. J. Iafrate, Phys. Lett. A **146**, 256 (1990).

[29] Y. Li, J. B. Krieger, M. R. Norman, and G. J. Iafrate, Phys. Rev. B **44**, 10437 (1991).

[30] Y. Li, J. B. Krieger, and G. J. Iafrate, Chem. Phys. Lett. **191**, 38 (1992).

[31] A. Heßelmann, A. W. Götz, F. Della Sala, and A. Görling, J. Chem. Phys. **127**, 054102 (2007).

[32] A. Makmal, S. Kümmel, and L. Kronik, J. Chem. Theory Comput. **5**, 1731 (2009).

[33] M. Hellgren and E. K. U. Gross, Phys. Rev. A **88**, 052507 (2013).

[34] S. V. Kohut, I. G. Ryabinkin, and V. N. Staroverov, J. Chem. Phys. **140**, 18A535 (2014).

[35] M. Städele, J. A. Majewski, P. Vogl, and A. Görling, Phys. Rev. Lett. **79**, 2089 (1997).

[36] H. O. Wijewardane and C. A. Ullrich, Phys. Rev. Lett. **100**, 056404 (2008).

[37] S. Kümmel, L. Kronik, and J. P. Perdew, Phys. Rev. Lett. **93**, 213002 (2004).

[38] M. Mundt, S. Kümmel, R. van Leeuwen, and P.-G. Reinhard, Phys. Rev. A **75**, 050501(R) (2007).

[39] M. Siegmund and O. Pankratov, Phys. Rev. B **83**, 045113 (2011).

[40] E. Engel, J. Chem. Phys. **140**, 18A505 (2014).

[41] S. Rigamonti, C. M. Horowitz, and C. R. Proetto, Phys. Rev. B **92**, 235145 (2015).

[42] C. M. Horowitz, C. R. Proetto, and S. Rigamonti, Phys. Rev. Lett. **97**, 026802 (2006).

[43] C. M. Horowitz, C. R. Proetto, and J. M. Pitarke, Phys. Rev. B **78**, 085126 (2008).

[44] C. M. Horowitz, L. A. Constantin, C. R. Proetto, and J. M. Pitarke, Phys. Rev. B **80**, 235101 (2009).

[45] C. M. Horowitz, C. R. Proetto, and J. M. Pitarke, Phys. Rev. B **81**, 121106 (2010).

[46] H. Luo, C. M. Horowitz, H.-J. Flad, C. R. Proetto, and W. Hackbusch, Phys. Rev. B **85**, 165133 (2012).

[47] E. Engel, Phys. Rev. B **89**, 245105 (2014).

[48] The argument behind the Taylor expansions of the exponent and the integrand in (18) can be given in an alternative fashion. If one first shifts the origin of the $\boldsymbol{k}$ integration to the point $\boldsymbol{q}$ and subsequently scales the momentum by $\sqrt{z}$, $\boldsymbol{k}' = (\boldsymbol{k} - \boldsymbol{q})\sqrt{z}$, one obtains $I = \int_{[1\mathrm{BZ}-\boldsymbol{q}]\times\sqrt{z}} \frac{d^2k}{(2\pi)^2} \Theta_{\boldsymbol{q}+\frac{\boldsymbol{k}}{\sqrt{z}},\alpha} A_{\boldsymbol{q}+\frac{\boldsymbol{k}}{\sqrt{z}},\alpha} \exp[-2\gamma_{\boldsymbol{q}+\frac{\boldsymbol{k}}{\sqrt{z}},\alpha} z + 2u \ln(z)/\gamma_{\boldsymbol{q}+\frac{\boldsymbol{k}}{\sqrt{z}},\alpha}]$, where $[1\mathrm{BZ} - \boldsymbol{q}] \times \sqrt{z}$ indicates the corresponding modification of the boundaries of the integration region. If now z becomes large, it is obvious that an expansion of $\gamma_{\boldsymbol{q}+\frac{\boldsymbol{k}}{\sqrt{z}},\alpha} = [(\boldsymbol{q} + \frac{\boldsymbol{k}}{\sqrt{z}})^2 - 2\epsilon_{\boldsymbol{q}+\frac{\boldsymbol{k}}{\sqrt{z}},\alpha}]^{1/2}$ for small $\boldsymbol{k}/\sqrt{z}$ is legitimate, and similarly for $A_{\boldsymbol{q}+\frac{\boldsymbol{k}}{\sqrt{z}},\alpha}$.

[49] Taking Eqs. (19), (39), and (40) together, one finds $\frac{d\boldsymbol{k}_\mathrm{h}}{ds}(s_q) \cdot \boldsymbol{q} = 0$. This is exactly what one observes in Fig. 3. Moreover, together with Eq. (40) this equation implies that $\mathbf{D}_{\boldsymbol{q}\alpha}$ is either parallel or antiparallel to $\boldsymbol{q}$.

[50] The same statement should apply to the common energy denominator/localized Hartree-Fock approximation [51,52]. The corresponding potential differs from the KLI approximation by the off-diagonal structure of the numerator of v_{shift}, Eq. (8). The off-diagonal structure leads to a double $\boldsymbol{k}$ integration, which, however, can be handled in exactly the same fashion as the single $\boldsymbol{k}$ integration in the numerator of (8).

[51] O. V. Gritsenko and E. J. Baerends, Phys. Rev. A **64**, 042506 (2001).

[52] F. Della Sala and A. Görling, J. Chem. Phys. **115**, 5718 (2001).